PAPER • OPEN ACCESS

Single Stage High Brightness LED Driver with Improved Power Quality

View the article online for updates and enhancements.

Single Stage High Brightness LED Driver with Improved Power Quality

Amit Agrawal[1,*]**, Ashish Shrivastava**[2]**, Kartick C Jana**[3]**, Sandeep Tripathi**[3]**, Amit Rai**[3]

[1]Department of Electrical & Electronics Engineering, ABES Engineering College, Ghaziabad, Uttar Pradesh, 201009, India
[2]Department of Electrical Engineering, Manipal University Jaipur, Rajasthan, 303007 India.
[3]Department of Electrical Engineering, Indian Institute of Technology (ISM), Dhanbad, Jharkhand, 826004, India.
E-mail: [*]amit.stm@gmail.com

Abstract. A single switch single stage 24watt power supply is presented to run a light emitting diode (LED) load. In this power supply, the Zeta converter is used to operate in continuous conduction mode (CCM) for maintaining desired output voltage. A proportional integral (PI) controller is also proposed in the feedback to make system stable. The need of proposed controller is justified from stability analysis of the system with the help of small signal average modeling. A simulation model of the proposed LED driver is also carried out in MATLAB/SIMLINK using sim-power toolbox environment for a universal ac input mains. The results confirm a constant current of 0.4amp at output with improved power quality parameters such as total harmonic distortion (THD) and power factor (PF). All outcomes lie under the limit of IEC 61000-3-2 standards that verifies the theoretical analysis.

Index Terms- Continuous Conduction Mode (CCM), LED Driver, Power Factor (PF), Small Signal Average (SSA) Modeling, THD, Stability, Zeta dc-dc Converter.

1. Introduction

In recent years, high brightness light emitting diode (HBLED) has become popular because of many benefits such as small size, long lifetime, high luminous efficiency, durability, environment friendliness due to nonappearance of mercury, flicker-less start, effortlessly dimmable, low maintenance, robust, vibration resistant and so on [1, 2]. Nowadays power LEDs are used in traffic lighting, automobile industry, aircraft lightings, railway signals, LCD backlight, biomedical apparatus, detective system, indoor and outdoor lightings etc [3]. Longer lifetime of LED compared with fluorescent lamp makes it economical to use even with its higher initial cost [4]. An LED driver uses a conversion stage that converts ac signal to dc signal which is required to operate an LED lamp. Converters with switching technology are most preferred among ac-dc conversion to run LEDs. These converters consist of rectifier and filter. The conventional converters have power quality issue in power factor and THD. The converter with the power factor corrector is used for the conversion by the researchers. For most marketable luminaries, power factor must to be at least 0.9 or more than that [5]. The proposed supply comes under class-D equipment and as per the norms of IEC 61000-3-2 the harmonic contents and power factor must be in the limit [6]. A suitable control scheme with PFC converter can make power factor good and efficiency high [7]. Single stage converters have more

benefit over the two stage converters for the low power applications because two stage structure increases the circuit cost, size and complication to design a suitable controller and reduces the overall efficiency [8, 9]. Commonly two stage converters need two independent power switches and two control circuits.

This paper focused on an inventive driving method for LED lamp and presented a novel single stage power supply with the benefits of the single stage converter, simplified control design, reduced number of components and lower cost. PI controller is designed to achieve system stability and SSA state space modeling [10] is applied to derive input to output and control to output transfer function. Frequency response of system loop gains is attained using MATLAB tool for justification of controller. For validation of theoretical analysis, a simulation is also performed in MATLAB/SIMULINK tool. Results shows 60volt, 0.4amp at output for universal ac supply from 90volt to 270volt and claims better power quality indices as PF and THD too. Topology is being operated at the switching frequency of 50kHz which helps to reduce the weight and size of passive components like inductor and capacitor. Input current THD and PF are maintained under the limit of standards given by IEC-61000-3-2 class D requirement.

2. Proposed topology: A PFC Zeta converter-based LED Driver

The block diagram of proposed LED driver is shown in Fig. 1. Here a diode bridge rectifier (DBR) is appended after input supply to generate rectified signal that enters further into PFC Zeta converter as input signal. This converter generates a constant dc voltage at output which is compared with the desired voltage and generates the error signal that works as input signal for PI controller. To generate pulse width modulated (PWM) signals, the PI controller's output is being compared with saw tooth wave signal having frequency of 50kHz. Further this signal drives an n-channel power MOSFET switch (S) with duty ratio D and switching frequency f_s. On the basis of switching period $T = 1/f_s$, the switch-on period is defined as $D*T$ and switch-off period is defined as $(1-D)*T$. When the switch M turns on, diode remains in reverse bias and the current ascends in the inductor L_1. When the switch turns off, the current flows through the freewheeling diode D due to its forward bias and descends for whole switch-off period $(1-D)*T$. The inductor current never comes to zero for any switching cycle in continuous conduction mode.
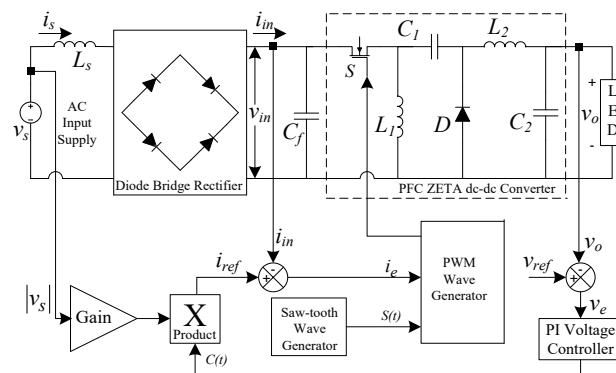

Figure 1. Block diagram of proposed LED driver

3. Components design of proposed LED Driver

The proposed LED driver is based on zeta converter operating in continuous conduction mode (CCM). Few points are listed below, which have been considered at the time of component's estimation to design this model.

- All components of proposed model are considered as ideal.
- LED load shows as a combination of pure resistor in series with dc battery and diode.

SV-TDFS -2018

IOP Conf. Series: Materials Science and Engineering **594** (2019) 012012

IOP Publishing

doi:10.1088/1757-899X/594/1/012012

- The dc link output capacitance (C_2) should be chosen as high enough so that a constant output voltage with less ripple contents can maintained at output for whole switching cycle.
- The switching frequency is chosen a higher value as compare to the frequency of input ac signal.
- Voltage across coupling capacitor (v_{C1}) is considered as maximum value of the applied input voltage signal.
- For estimation of inductors value, change in ripple current is allowed up to 100% of the average load current.

Components value is calculated with help of standard equations discussed below. The value of duty cycle and critical value of inductances L_1 and L_2 are defined by equation (1) and (2) [11].

$$D = v_o/(v_i + v_o) \tag{1}$$

$$L_{1(critical)} = L_{2(critical)} = (1-D)v_o/2Df_sI_o \tag{2}$$

The value of coupling capacitor and output capacitor is designed with help of below expressions that is based on ripple content [11].

$$C_1 = i_o D/f_s \Delta v_{C1} \tag{3}$$

$$C_2 = i_o/2\omega \Delta v_{C2} \tag{4}$$

Here, v_i is the maximum value of ac mains input voltage, ω is the input supply frequency, v_o is output voltage, i_o is average output load current, the symbol D is used as duty cycle, f_s is switching frequency of the switch device, Δv_{C1} is the ripple voltage of capacitor C_1 and Δv_{C2} is the ripple voltage of capacitor C_2. Parameter and component's value are calculated and presented in Table 1 with help of equation (1), (2), (3) and (4) to get desired output voltage.

Table 1. Parameter and Component of Proposed Model

Parameter and Component	Calculated Value	Selected Value
Supply voltage (v_s)	--	220volt
Supply frequency (ω)	--	50Hz
Output voltage (v_o)	--	60volt
Switching frequency (f_s)	--	50kHz
Maximum value of coupling capacitor voltage (v_{c1})	311.08volt	311.08volt
Ripple voltage of coupling capacitor $\Delta v_{c1} = 12\%$ of v_{c1}	37.33volt	37.33volt
Ripple voltage of dc link output capacitor $\Delta v_{c2} = 3\%$ of v_{c2}	1.8volt	1.8volt
Value of duty cycle for ac mains input of 270volt	0.135	--
Value of duty cycle for ac mains input of 90volt	0.320	--
Duty cycle (D)	--	0.161
Averaged Load Current I_o	0.4amp	0.4amp
Critical value of inductor L_1	6.77mH	10mH
Critical value of inductor L_2	6.77mH	10mH
Average inductor current (I_{L_1})	0.12amp	0.12amp
Average inductor current (I_{L_2})	0.40amp	0.40amp
Coupling capacitor C_1	49.93nF	50nF
Output capacitor C_2	353.53μF	400μF
V_{OSC} (Oscillator voltage)	--	4.5volt
v_{ref} (Reference voltage)	--	1.5volt

4. Small Signal Average Model

The diagram of Zeta converter is showing the mathematical description of the real system behavior in Fig.1. The SSA state space methodology is a universal tool which is easily applicable for the detail analysis of the complex structures of the converter in CCM or DCM [12, 13]. With help of this

method, the linear averaged time invariant model and its derived mathematical results is achieved. All state matrices are derived and written below by using Kirchhoff's voltage and current laws for two operating modes switch-on and switch-off.

$$A_1 = \begin{bmatrix} 0 & 0 & 0 & 0 \\ 0 & 0 & 1/L_2 & -1/L_2 \\ 0 & -1/C_1 & 0 & 0 \\ 0 & 1/C_2 & 0 & -1/RC_2 \end{bmatrix},$$

$$A_2 = \begin{bmatrix} 0 & 0 & -1/L_1 & 0 \\ 0 & 0 & 0 & -1/L_2 \\ 1/C_1 & 0 & 0 & 0 \\ 0 & 1/C_2 & 0 & -1/RC_2 \end{bmatrix},$$

$$B_1 = \begin{bmatrix} 1/L_1 \\ 1/L_2 \\ 0 \\ 0 \end{bmatrix},$$

$$B_2 = \begin{bmatrix} 0 \\ 0 \\ 0 \\ 0 \end{bmatrix} \tag{5}$$

The state-space average equilibrium matrixes are calculated and written below.

$$A = DA_1 + (1-D)A_2$$

$$A = \begin{bmatrix} 0 & 0 & (D-1)/L_1 & 0 \\ 0 & 0 & D/L_1 & -1/L_2 \\ (1-D)/C_1 & -D/C_1 & 0 & 0 \\ 0 & 1/C_2 & 0 & -1/RC_2 \end{bmatrix} \tag{6}$$

$$B = DB_1 + (1-D)B_2$$

$$B = \begin{bmatrix} D/L_1 \\ D/L_2 \\ 0 \\ 0 \end{bmatrix} \tag{7}$$

To build a small signal ac model at an operating point, the duty ratio is considered as

$$d(t) = D + \hat{d}(t) = D + d_m \sin \omega t \tag{8}$$

Where $_D$ and d_m are the constant and $d_m << D$.

The small signal ac model can be achieved using equation mentioned below.

$$d\dot{x}(t)/dt = A\hat{x}(t) + B\hat{v}(t) + \{(A_1 - A_2)X + (B_1 - B_2)V\}\hat{d}(t) \tag{9}$$

The small signal ac state space model is written below by putting all value of matrix in equation (22).

$$\begin{bmatrix} d\hat{i}_{L1}(t)/dt \\ d\hat{i}_{L2}(t)/dt \\ d\hat{v}_{C1}(t)/dt \\ d\hat{v}_{C2}(t)/dt \end{bmatrix} = \begin{bmatrix} 0 & 0 & (D-1)/L_1 & 0 \\ 0 & 0 & D/L_1 & -1/L_2 \\ (1-D)/C_1 & -D/C_1 & 0 & 0 \\ 0 & 1/C_2 & 0 & -1/RC_2 \end{bmatrix} \begin{bmatrix} \hat{i}_{L1} \\ \hat{i}_{L2} \\ \hat{v}_{C1} \\ \hat{v}_{C2} \end{bmatrix} + \begin{bmatrix} D/L_1 \\ D/L_2 \\ 0 \\ 0 \end{bmatrix} \hat{v}_i(t)$$

$$+ \left\{ \begin{bmatrix} 0 & 0 & 1/L_1 & 0 \\ 0 & 0 & 1/L_2 & 0 \\ -1/C_1 & -1/C_1 & 0 & 0 \\ 0 & 0 & 0 & 0 \end{bmatrix} \begin{bmatrix} I_{L1} \\ I_{L2} \\ V_{C1} \\ V_{C2} \end{bmatrix} + \begin{bmatrix} 1/L_1 \\ 1/L_2 \\ 0 \\ 0 \end{bmatrix} V_i \right\} \hat{d}(t) \tag{10}$$

After taking the Laplace transform, model can be written in the form of equations also as below.

$$sL_1 \hat{I}_{L1}(s) = (D-1)\hat{V}_{C1}(s) + D\hat{V}_i(s) + V_{C1}\hat{d}(s) + V_i \hat{d}(s) \tag{11}$$

$$sL_2 \hat{I}_{L1}(s) = D\hat{V}_{C1}(s) - \hat{V}_{C2}(s) + D\hat{V}_i(s) + V_{C1}\hat{d}(s) + V_i \hat{d}(s) \tag{12}$$

$$sC_1 \hat{V}_{C1}(s) = (1-D)\hat{I}_{L1}(s) - D\hat{I}_{L2}(s) + (I_{L1} + I_{L2})\hat{d}(s) \tag{13}$$

$$sRC_2 \hat{V}_{C2}(s) = R\hat{I}_{L2}(s) - \hat{V}_{C2}(s) \tag{14}$$

Output voltage (v_o) follows the output capacitor voltage (v_{C2}). With help of equation (11) to (14), output voltage response in frequency domain is achieved and written below.

$$\hat{v}_{C2}(s) = \frac{\begin{aligned} &(RL_2 D^2(1-D) + RL_1 D(1-D)^2 + RL_1^2 C_1 D s^2)\hat{V}_i(s) + ((RDL_2(1-D) + RL_1(1-D)^2 \\ &+ RC_1 L_1^2 s^2)(V_{C1} + V_{in}) - RDL_1 L_2(I_{L1} + I_{L2})s)\hat{d}(s) \end{aligned}}{\begin{aligned} &RL_1^2 L_2 C_1 C_2 s^4 + L_1^2 L_2 C_1 s^3 + RL_1(L_1 C_1 + L_2 C_2(D^2 - D + 1))s^2 \\ &+ L_1 L_2(D^2 - D + 1)s + RL_1(1-D)^2 \end{aligned}} \tag{15}$$

Control to output transfer function ($G_{vd}(s)$) of model is written below using equation (15).

$$G_{vd}(s) = \left| \hat{V}_o(s)/\hat{d}(s) \right|_{\hat{V}_i(s)=0}$$

$$G_{vd}(s) = \frac{(RDL_2(1-D) + RL_1(1-D)^2 + RC_1 L_1^2 s^2)(V_{C1} + V_i) - RDL_1 L_2(I_{L1} + I_{L2})s}{\begin{aligned} &RL_1^2 L_2 C_1 C_2 s^4 + L_1^2 L_2 C_1 s^3 + RL_1(L_1 C_1 + L_2 C_2(D^2 - D + 1))s^2 \\ &+ L_1 L_2(D^2 - D + 1)s + RL_1(1-D)^2 \end{aligned}} \tag{16}$$

After putting component's value in equation (16), the mathematical value of the control to output transfer function is written by equation (17).

$$G_{vd}(s) = \frac{4.7*10^{-7} s^2 - 1.3*10^{-3} s + 783}{3*10^{-15} s^4 + 5*10^{-14} s^3 + 5.2*10^{-6} s^2 + 8.6*10^{-5} s + 1.1} \tag{17}$$

The transfer function (TF) of the PWM block is estimated below.

$$G_{PWM}(s) = \left| \hat{d}(s)/\hat{V}_e(s) \right| = 1/V_{osc} \tag{18}$$

The loop gain of the model $G(s)$ can be achieved as below.

$$G(s) = G_{vd}(s)*G_{PWM}(s)*v_{ref}/v_{dc}$$

Mathematical expression of $G(s)$ is written below by putting all component's value from Table 1 in above equation.

$$G(s) = \frac{7.05*10^{-7} s^2 - 1.95*10^{-3} s + 1175}{8.1*10^{-13} s^4 + 1.35*10^{-11} s^3 + 1.4*10^{-3} s^2 + 2.32*10^{-2} s + 297} \tag{19}$$

5. Stability Analysis of System in absence of Controller

System loop gain of proposed model is achieved with help of SSA modeling in section 4. Bode plot is taken out from MATLAB tool and shown in Fig. 2 to check system stability. Gain margin of 21.5dB and phase margin of 1.06˙ are observed from frequency response. For a practical system, phase margin must be greater than 45˙ to fulfill stability criterion. It clearly demands a control scheme in feedback discussed in next section.
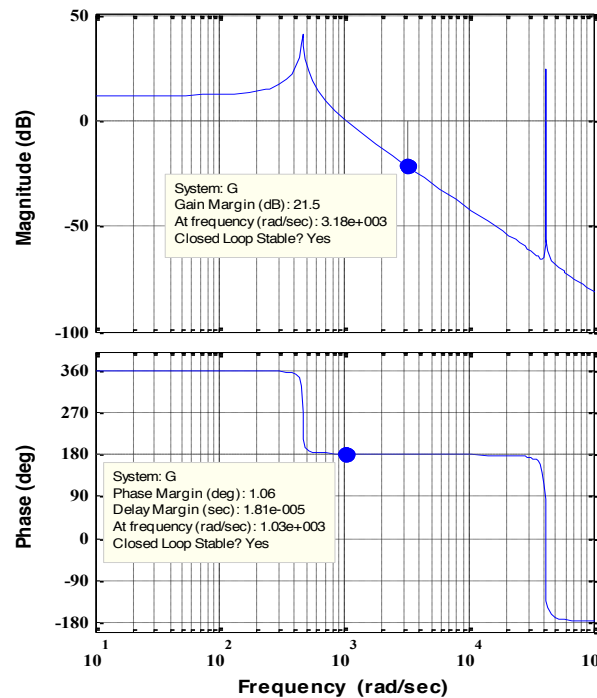

Figure 2. Bode Plot of transfer function $G(s)$

6. Feedback System

A controller is design in this section to achieve stability criterion. It sends optimize input to PWM wave generator which changes the duty cycle accordingly and controls the ON time of MOSFET switch. Component's design and stability analysis is explained below.

6.1. PI Controller

Fig. 3 shows the schematic circuit of PI controller network which is working as a voltage controller. It senses the output dc voltage (v_o) and compares with reference voltage (v_{ref}) to generate error voltage signal (v_e).

$$v_e = v_{ref} - v_o$$

According to error voltage, controller sends signal to PWM block at every sampling instant. The value at n^{th} sampling instant is defined by equation (20).

$$I_c(n) = I_c(n-1) + K_p\{v_e(n) - v_e(n-1)\} + K_i v_e(n) \tag{20}$$

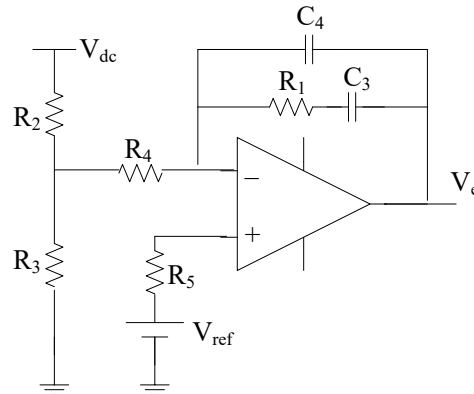Where, K_p and K_i are the proportional and integral gains respectively.

Figure 3. Network of PI Controller

6.2. PWM signal generation

This block compares both signal coming from PI controller and saw-tooth wave generator. It controls the width of pulse which changes the on time of switch. Saw-tooth wave generator sends a fixed frequency carrier signal.

If $K_c * I_c(n)>$ carrier signal, then $M=1$ else $M = 0$.

6.3. Component's design of PI Controller

The transfer function of controller network is defined by equation (35).

$$C(s) = (1 + sR_1C_3)/sR_2.((C_3 + C_4) + sR_1C_3C_4) \tag{21}$$

All components are calculated by using standard formulas given below where bandwidth (BW) and ΔV_{ovp} are chosen 20Hz and 3volt respectively [14].

$$R_2 = \Delta V_{ovp}/30\mu A \tag{22}$$

$$R_3 = R_2 v_{ref}/(v_o - v_{ref}) \tag{23}$$

$$R_1 = R_3 v_{ref}/(V_{osc} - v_{ref}) \tag{24}$$

$$f_o = 1/(2\pi\sqrt{L_2C_2}) \tag{25}$$

$$f_z = .75f_o \tag{26}$$

$$C_3 = 1/(2\pi R_1 f_z) \tag{27}$$

$$C_4 = 1/(2\pi(R_2\|R_3)BW) \tag{28}$$

Mathematical expression of controller is written below by putting all components value in equation (21).

$$C(s) = 7.6*10^{-3}s + 1/(3.45*10^{-3}s^2 + 1.86s) \tag{29}$$

6.4. Stability Analysis of Model with proposed control scheme

A controller is suggested and designed above with transfer function $C(s)$. The new loop gain of system ($G_c(s)$) is defined by equation (44) for further stability analysis.

$$G_c(s) = G(s)*C(s) \tag{30}$$

Mathematical expression is written with help of equation (19) and (30).

$$G_c(s) = \frac{5.358*10^{-9}s^3 - 1.412*10^{-5}s^2 + 8.928s + 1175}{s(2.795*10^{-15}s^5 + 1.553*10^{-12}s^4 + 4.83*10^{-6}s^3 + 2.684*10^{-3}s^2 + 1.068s + 552.4)} \tag{31}$$

Bode plot is taken out from MATLAB again for equation (31) and shown in Fig 4 respectively. Gain margin of 10.7dB and phase margin of 90.7˙ clearly defend the system stability.
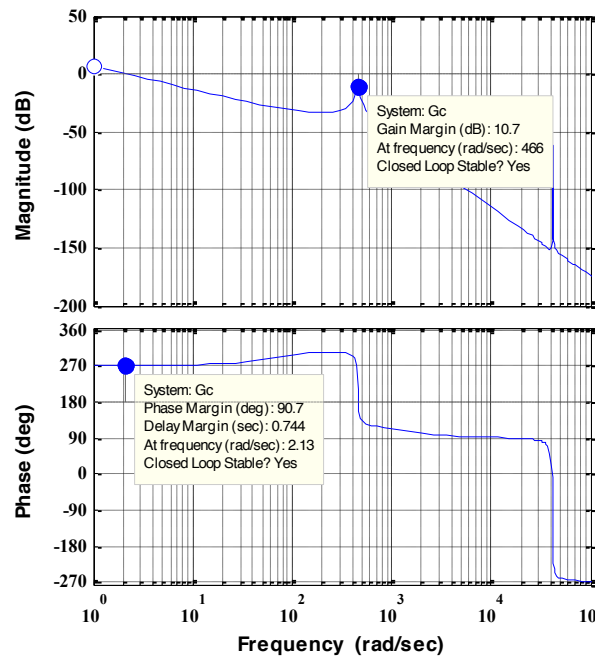
Figure 4. Bode plot of transfer function $G_c(s)$

7. Simulated Model in MATLAB

The proposed model is simulated in the platform of MATLAB and shown in Fig. 5. Input supply is being converted into full wave rectified signal using DBR. Further a PFC block is used to generate a constant voltage at output. It is based on zeta topology operating in CCM. PI controller is generating signal according to difference between output and desired signal. A saw tooth wave generator is used to send a signal of frequency 50kHz to PWM block which controls the on time of MOSFET switch. Value of all the components for proposed model has been designed and selected properly to maintain better power quality within the limits of international standards.
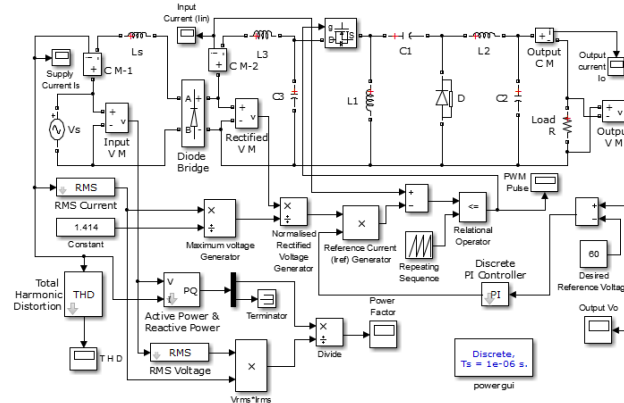

Figure 5. Simulated model of proposed power supply

8. Results and Discussion

The simulation result shows that 60volt is maintained at output for 220volt supply of input. The waveform of supply current (I_s), supply voltage (V_s), output current (I_o) and output voltage (V_o), inductor current (I_{Li}) is extracted at 220volt and shown in Fig. 6. In Table 2, the power quality parameters are written at different supply voltage. The power factor is achieved more than 0.91 for

wide range of supply voltage (90volt-270volt) and the THD is maintained from 0.25% to 0.72%. It claims that the proposed model is a good choice as an LED driver with high power quality parameters.

Table 2. Performance Parameters of Simulated Power Supply Based on Zeta Converter

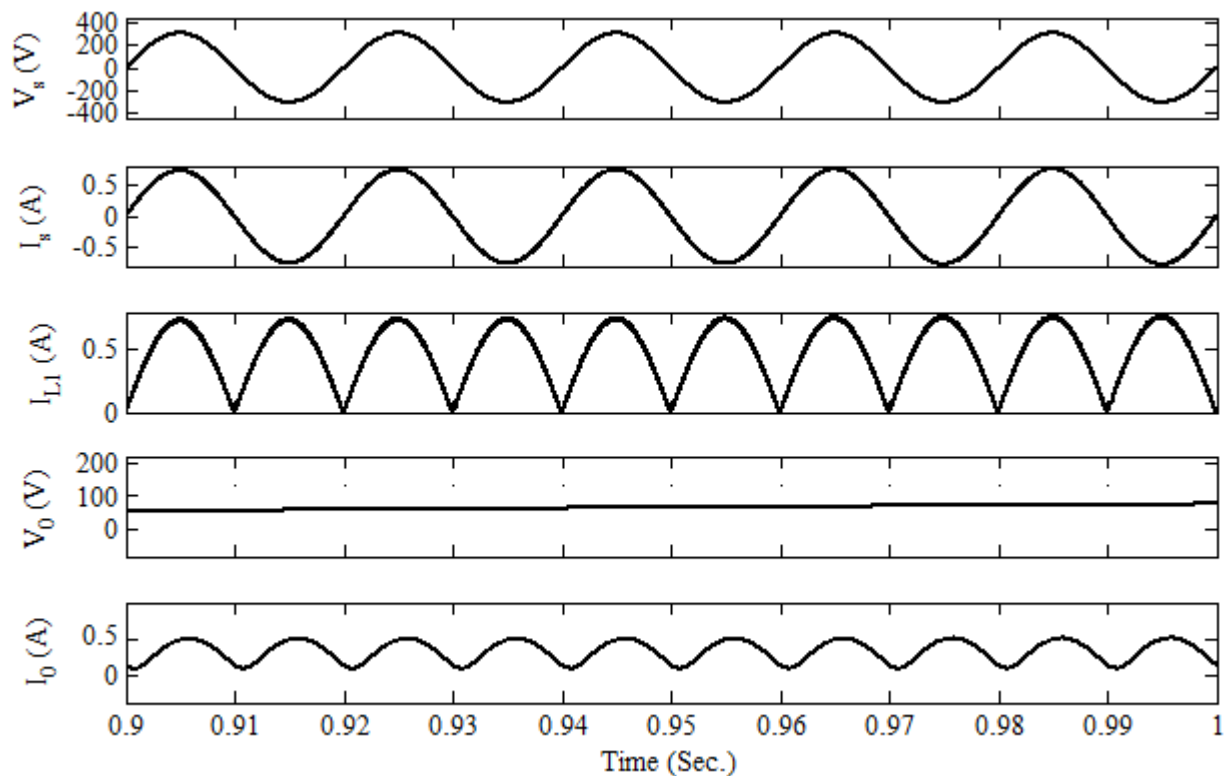| Supply Voltage (V_s), V	Input Current (I_s), A	Load Voltage (V_o), V	Load Current (I_o), A	Power Factor (PF)	% THD
90	0.26	59.8	0.39	.91	0.72
150	0.17	60.2	0.42	.93	0.54
220	0.13	60.3	0.44	.98	0.25
270	0.10	61.2	0.40	.91	0.70

Figure 6. Waveforms of Supply current, voltage, inductor current, output voltage and current

9. Conclusion

A model of 24watt, 60volt power supply based on Zeta topology operating in CCM is presented to run a LED light. State space modeling is applied in this topology and loop gain is achieved to examine the system stability. PI controller is also designed and applied with feedback to make system stable. Stability analysis is done in detail with help of Bode, Nyquist, and Polar plot of loop gains drawn in MATLAB tool. The simulation of proposed LED driver is performed in sim power toolbox to justify theoretical and mathematical analysis. Its result shows a constant current rating of 0.4amps at output with improved power quality parameter such as the THD and PF for universal ac input mains. Improved PF and reduced harmonics of ac mains input are under the limit of IEC 61000-3-2 Class D equipment.

References

[1]   C. Y. Wu, T. F. Wu, J. R. Tsai, Y. M. Chen, and C. C. Chen, "Multistring LED backlight driving system for LCD panels with color sequential display and area control," *IEEE Trans. Ind. Electron.*, vol. 55, no. 10, pp. 3791–3800, Oct. 2008.

[2]   L. Xingming and Z. Jing, "An intelligent driver for light emitting diode street lighting," in *Proc. World Automation Congr. (WAC)*, 2008, pp. 1–5.

[3]   C. C. Chen, C.-Y. Wu, and T.-F. Wu, "LED back-light driving system for LCD panels," in *Proc. IEEE Appl. Power Electron. Conf. Expo.*, Mar. 2006, pp. 381–385.

[4]   Robert S. Simpson, "Lighting Control Technology and Applications," Focal Press, Burlington, MA, USA, 2003.

[5]   B. Weir and F. Cathell, "LED streetlight demands smart power supply," *Power Electron. Technol.*, vol. 34, no. 2, pp. 34–39, Feb. 2008.

[6]   Limits for Harmonic Current Emissions, *International Electrotechnical Commission Standard,* IEC-61000-3-2, 2004.

[7]   H. Broeck, G. Sauerl̈ander, and M. Wendt, "Power driver topologies and control schemes for LEDs," in *Proc. IEEE APEC 2007*, pp. 1319–1325.

[8]   Z.Ye, F.Greenfeld, and Z. Liang, "A topology study of single-phase offline ac/dc converters for high brightness white LED lighting with power factor pre-regulation and brightness dimmable feature," in *Proc. 34th Annu. Conf. IEEE Ind. Electron.*, Nov.10–13, 2008, pp. 1961–1967.

[9]   Amit Agrawal, Ashish Shrivastava, Kartick C. Jana, "A Universal Input, Single Stage AC-DC LED Driver for an Auditorium Light", *Journal of circuit, system and computers*, vol. 28, no. 2, Feb 2019.

[10] G. Gatto, I. Marongiu, A. Mocci, A. Serpi, "An improved averaged model for boost dc-dc converters" in Proc. IECON, 412– 417, Vienna, 2013.

[11] Ashish Shrivastava and Bhim Singh, "Power factor-corrected DCM-based electronic ballast," *Electrical Engineering*, vol. 95, no. 4, pp. 403-411, Dec 2013.

[12] R. W. Erickson, *Fundamentals of Power Electronics*, 1st ed., New York: Chapman and Hall, 1997.

[13] Amit Agrawal, Ashish Shrivastava, Kartick C. Jana, "Uniform Model and Analysis of PWM DC-DC Converter for Discontinuous Conduction Mode", *IETE journal of Research*, Vol. 64, issue-4, 2018, pp. 569-581.

[14] Bhim Singh and Ashish Shrivastava, "Buck converter based power supply design for low power light emitting diode lamp lighting," *IET Power Electronics*, vol. 7, no. 4, pp. 946-956, 2014.